Correlation between electronic structure and energy band in Eu-doped $CuInTe_2$ semiconductor compound with chalcopyrite structure*

Tai Wang(王泰), Yong-Quan Guo(郭永权)†, and Shuai Li(李帅)

School of Energy Power and Mechanical Engineering, North China Electric Power University, Beijing 102206, *China*

(Received 5 April 2017; revised manuscript received 15 June 2017; published online 20 August 2017)

The Eu-doped Cu(In, Eu)Te_2 semiconductors with chalcopyrite structures are promising materials for their applications in the absorption layer for thin-film solar cells due to their wider band-gaps and better optical properties than those of $CuInTe_2$. In this paper, the Eu-doped $CuInTe_2$ ($CuIn_{1-x}Eu_xTe_2$, $x = 0$, 0.1, 0.2, 0.3) are studied systemically based on the empirical electron theory (EET). The studies cover crystal structures, bonding regularities, cohesive energies, energy levels, and valence electron structures. The theoretical values fit the experimental results very well. The physical mechanism of a broadened band-gap induced by Eu doping into $CuInTe_2$ is the transitions between different hybridization energy levels induced by electron hopping between s and d orbitals and the transformations from the lattice electrons to valence electrons for Cu and In ions. The research results reveal that the photovoltaic effect induces the increase of lattice electrons of In and causes the electric resistivity to decrease. The Eu doping into $CuInTe_2$ mainly influences the transition between different hybridization energy levels for Cu atoms, which shows that the 3d electron numbers of Cu atoms change before and after Eu doping. In single phase $CuIn_{1-x}Eu_xTe_2$, the number of valence electrons changes regularly with increasing Eu content, and the calculated band gap E_g also increases, which implies that the optical properties of Eu-doped $CuIn_{1-x}Eu_xTe_2$ are improved.

Keywords: $CuIn_{1-x}Eu_xTe_2$, EET, solar cells, valence electronic structures, band gap

PACS: 31.15.bu, 88.40.jn, 88.40.H–, 42.70.Nq **DOI:** 10.1088/1674-1056/26/10/103101

1. Introduction

I–III–VI_2 semiconductors with chalcopyrite structures have received a great deal of attention due to their excellent optical properties such as visible and infrared light-emitting diodes, infrared detector, etc.[1–8] Since the band gap E_g of chalcopyrite semiconductors covers most of the energy spectra for the visible light (1 eV–3 eV), the maximum absorption of the solar spectrum can be utilized for the energy conversion and cause these chalcopyrites to develop into the possible substrates for the fabrication of optoelectronic devices.[2,9–17] The solar cells based on $CuInSe_2$ and $CuInS_2$ have already reached efficiencies of 18.8% and 12%, respectively.

Since $CuInTe_2$ is a direct band gap semiconductor, in order to minimize the requirements for minority carrier diffusion lengths, it can be made as either n- or p-type semiconductor with a variety of potentially low-cost homojunction and heterojunction applications as an alternative to monocrystalline and polycrystalline silicon technology.[11,12,16,18–21] Some relevant studies have been reported. Gonzalez and Rincón reported the optical absorption and phase transitions of $CuInTe_2$.[3] Mi analyzed systematically the optical properties of $CuInTe_2$ by the first principle based on the electronic band structures.[22] Li *et al.* have calculated the band structure of $CuInTe_2$ by the first principle for explaining the mechanism of the thermoelectric property based on electronic structure.[23] However, the first principle approach needs to introduce many approximations according to the atomic structure of the material, and its calculus calculation process is more complicated.

Rare earth ions doping into the semiconductor could enhance the luminescent and fluorescent properties due to its specific 4f electronic structure and unique optical properties such as high quantum efficiencies of absorption light at short wavelength and subsequent emission light at long wavelength.[24–28] The carrier concentration of Cd-doped $CuInTe_2$ has been reported by Cheng *et al.*[18] The goal of our study on rare earth doping in $CuInTe_2$ material is to study the essential photoelectric mechanism of an Eu-doped $CuInTe_2$ semiconductor with chalcopyrite structure and investigate the correlation between their electronic structures and hybridization energy levels. In this study, empirical electron theory (EET) has been used to study the valance electric structures and band gap of Eu-doped $CuInTe_2$ since it has the advantage of being a simple calculation model without any integral and differential modes and much more parameters.

2. Theoretical models

The EET includes four basic hypotheses for the atomic hybridization states and one calculation method, so-called the

*Project supported by the National Natural Science Foundation of China (Grant No.1 1274110).

†Corresponding author. E-mail: yqguo@ncepu.edu.cn

© 2017 Chinese Physical Society and IOP Publishing Ltd

bond length difference (BLD), where the atomic valence and dimensional characteristics are the two key factors to characterize the valence states in a solid molecule.[27–29] The four basic hypotheses and the bond length difference (BLD) have been systematically illustrated in Refs. [30]–[32], and a conclusion has been obtained that the covalence electron number originating from all bonding atoms is equal to the total number of valence electronic pairs formed by all covalent bonds in the system. The absolute difference $|\Delta D|$ between the theoretical and the experimental bond length is defined as a criterion for checking the reasonability for determining the final hybridization state with BLD. If the $|\Delta D|$ is less than 0.05 Å, the calculations are acceptable.[28,33]

The number of equivalent bonds for one bond in EET is defined as[28]

$$I_\alpha = I_M I_S I_K, \tag{1}$$

where I_α is the number of equivalent bonds of the α bond, I_M is the number of atoms in the molecular formula, and I_S is the coordination number of atoms for the α bond. For I_K, if the bond forms in the same type of atom such as Cu–Cu, In–In, Te–Te or (Eu,In)–(Eu,In), I_K is equal to 1; if not, I_K is equal to 2.[28] In the Appendix A, the numbers of s, p, and d electrons are listed in the hybridization tables of Cu, In, Te, and Eu. Besides, the model of cohesive energy is also supplied.

2.1. Results and discussion

In this paper, the Eu content-dependent valence electronic structures and cohesive energies for $CuIn_{1-x}Eu_xTe_2$ have been analyzed.

2.2. Structural parameters

According to our previous study of the structures and electric transports of Eu-doped $CuIn_{1-x}Eu_xTe_2$ (CIET),[25] Eu-doping into $CuInTe_2$ still stabilizes the tetragonal chalcopyrite structure, and its lattice parameters and atomic occupations are listed in Table 1.[25]

Table 1. Lattice parameters and atom occupation of $CuIn_{1-x}Eu_xTe_2$.

Compound	$CuInTe_2$	$CuIn_{0.9}Eu_{0.1}Te_2$	$CuIn_{0.8}Eu_{0.2}Te_2$	$CuIn_{0.7}Eu_{0.3}Te_2$
Space group	*I*-42*d*	*I*-42*d*	*I*-42*d*	*I*-42*d*
a/Å	6.1910	6.1912	6.1899	6.1898
c/Å	12.4077	12.4073	12.4056	12.4091
Cu(4a)	(0, 0, 0)	(0, 0, 0)	(0, 0, 0)	(0, 0, 0)
In/Eu(4b)	(0, 0, 1/2)	(0, 0, 1/2)	(0, 0, 1/2)	(0, 0, 1/2)
Te(8d)	(0.21991, 1/4, 1/8)	(0.21819, 1/4, 1/8)	(0.22156, 1/4,1/8)	(0.21626, 1/4,1/8)

2.3. Crystal structure and strong bonds

According to the structural parameters of CIET compounds in Table 1, the structural frame is drawn using the Diamond software as shown in Fig. 1. The experimental bond distances and atomic coordination numbers can be measured, and the number of equivalent bonds I_α can be calculated from Eq. (1). The related bonding parameters are supplied in Tables 2–5. The bonds are corresponding to the first most and the second most strongest bonds between Cu–Te and Te–In(Eu) as also shown in Fig. 1.

Table 2. Bonding rule of $CuInTe_2$.

Bond order	Bonding atom	I_α	Bond length/Å	Bond order	Bonding atom	I_α	Bond length/Å
1	Cu–Te	8	2.5797	6	Cu–In	8	4.3822
2	In-Te	8	2.7943	7	Cu–Cu	4	4.3822
3	Te–Te	4	4.1227	8	In–In	4	4.3822
4	Te–Te	8	4.2568	9	Te–Te	8	4.5196
5	Cu–In	8	4.3777	10	Te–Te	4	4.6486

Table 3. Bonding rule of $CuIn_{0.9}Eu_{0.1}Te_2$.

Bond order	Bonding atom	I_α	Bond length/Å	Bond order	Bonding atom	I_α	Bond length/Å
1	Cu–Te	8	2.5741	6	Cu–In, Eu	8	4.3822
2	In, Eu–Te	8	2.8009	7	Cu–Cu	4	4.3822
3	Te–Te	4	4.1008	8	In, Eu–In, Eu	4	4.3822
4	Te–Te	8	4.2500	9	Te–Te	8	4.5278
5	Cu–In, Eu	8	4.3788	10	Te–Te	4	4.6674

Table 4. Bonding rule of $CuIn_{0.8}Eu_{0.2}Te_2$.

Bond order	Bonding atom	I_α	Bond length/Å	Bond order	Bonding atom	I_α	Bond length/Å
1	Cu–Te	8	2.5846	6	Cu–In, Eu	8	4.3815
2	In, Eu-Te	8	2.7874	7	Cu–Cu	4	4.3815
3	Te–Te	4	4.1355	8	In, Eu–In, Eu	4	4.3815
4	Te–Te	8	4.2626	9	Te–Te	8	4.5110
5	Cu–In, Eu	8	4.3769	10	Te–Te	4	4.6326

Table 5. Bonding rule of $CuIn_{0.7}Eu_{0.3}Te_2$.

Bond order	Bonding atom	I_α	Bond length/Å	Bond order	Bonding atom	I_α	Bond length/Å
1	Cu–Te	8	2.5676	6	Cu–In, Eu	8	4.3821
2	In, Eu-Te	8	2.8081	7	Cu–Cu	4	4.3821
3	Te–Te	4	4.0922	8	In, Eu–In, Eu	4	4.3821
4	Te–Te	8	4.2423	9	Te–Te	8	4.5368
5	Cu–In, Eu	8	4.3768	10	Te–Te	4	4.6815

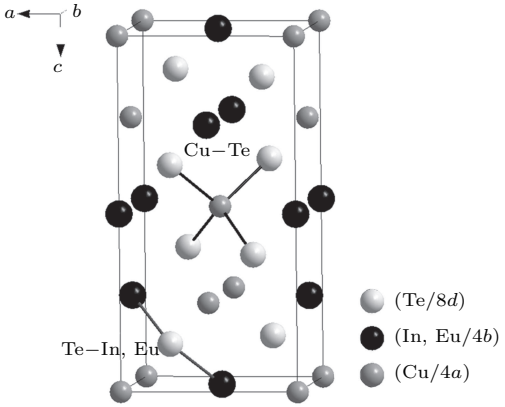


Fig. 1. Crystal structures of CIET series compounds with chalcopyrite structures.

2.4. Energy at various valence electron hybridization states

For studying the relationships between valence electron hybridization state and energy for $CuIn_{1-x}Eu_xTe_2$ semiconductors, the hybridizing parameters, which cover the covalent electrons of s, p, d, lattice electron, dumb electrons, and magnetic electrons in h and t states for Cu, In, Eu, and Te, could be determined using the BLD method with the empirical criterion $|\Delta D| \leq 0.05$ Å based on the hybrid states of Cu, In, Eu, and Te in Appendix A.

The theoretical model of hybridization energy is presented in the supplement section. The hybridization parameters determined with BLD are selected as the initial parameters for calculating hybridization energies; if the energy difference between two hybridization states could fit the light absorption band-gap, the solution is acceptable. $CuInTe_2$ is taken as a typical calculation example, the hybridization states of the valence electron so-called valence structure are supplied in Table 6, where I denotes the equivalent bond number, $\overline{D}_{uv}(n_\alpha)$ and $D_{uv}(n_\alpha)$ refer to the calculated bond distance and experimental bond distance, respectively, and ΔD is the difference between $\overline{D}_{uv}(n_\alpha)$ and $D_{uv}(n_\alpha)$, n_α denotes the number of valence electronic pairs distributed in each bond, and $f = (\Delta D/D_{uv}(n_\alpha))\,\%$ is the relative error.

Table 6. Valence electronic structure of CuInTe2.

I	$\overline{D}_{uv}(n_\alpha)$/Å	$D_{uv}(n_\alpha)$/Å	ΔD/Å	n_α	f/%
8	2.5727	2.5797	–0.0070	1.4628	–0.2600
8	2.7873	2.7943	–0.0070	0.3392	–0.2800
4	4.1158	4.1228	–0.0070	0.0080	–0.1700
8	4.2498	4.2568	–0.0070	0.0052	–0.1700
8	4.3707	4.3777	–0.0070	0.0025	–0.1600
8	4.3752	4.3822	–0.0070	0.0024	–0.1600
4	4.3752	4.3822	–0.0070	0.0011	–0.1600
4	4.3752	4.3822	–0.0070	0.0052	–0.1600
8	4.5126	4.5196	–0.0070	0.0022	–0.1600
4	4.6416	4.6486	–0.0070	0.0014	–0.1600

Based on the determined results of valence electron structures, the related hybridization energies are calculated and the results are listed in Tables 7–10. Owing to the multi-solution in the calculation, the observed band-gap is taken as a criterion for selecting the reasonable solution, if the energy difference between two hybridization states could fit the band-gap well (the fitting error is within 10%), the solution is acceptable.

Table 7. Calculated values of hybrid state and hybrid energy of $CuInTe_2$.

σ	Cu	In	Te	Hybrid energy/kcal·mol^{-1}
1	9	10	1	314.6231
2	11	10	1	318.1892
3	13	10	1	342.8708
4	17	9	1	319.9201
5	17	10	1	354.2455

Table 8. Calculated values of hybrid state and hybrid energy of $CuIn_{0.9}Eu_{0.1}Te_2$.

σ	Cu	In	Te	Eu	Hybrid energy/kcal·mol^{-1}
1	13	9	1	1	304.6148
2	13	10	1	1	334.8437
3	15	9	1	1	312.1502
4	15	10	1	1	342.6048
5	17	9	1	1	315.5869

Table 9. Calculated values of hybrid state and hybrid energy of $CuIn_{0.8}Eu_{0.2}Te_2$.

σ	Cu	In	Te	Eu	Hybrid energy/kcal·mol^{-1}
1	13	10	1	1	329.5607
2	15	9	1	1	309.9747
3	15	10	1	1	337.321
4	17	9	1	1	313.4229
5	17	10	1	1	340.8581

Table 10. Calculated values of hybrid state and hybrid energy of $CuIn_{0.7}Eu_{0.3}Te_2$.

σ	Cu	In	Te	Eu	Hybrid energy/kcal·mol^{-1}
1	13	10	1	1	319.5803
2	15	9	1	1	303.9720
3	17	7	1	1	281.7519
4	17	9	1	1	307.3936
5	17	10	1	1	330.7531

2.5. Analyses and discussion of CIET

For studying the physical mechanism for CIET photovoltaic characteristics, the changes of valence electron structure induced by the photoelectric conversion effect, which include the electron transitions between various orbits and electron transformation between the valence electron and lattice electron, should be taken into account. The light absorption causes the increase of energy of the CIET system, and thus changes the relative electron structure. The electron numbers, which are distributed in various orbitals and lattice space, change due to the electron hopping between various orbitals or electron transformation from valence electron to lattice electron. The open voltage increases with lattice electron increasing.

For $CuIn_{1-x}Eu_xTe_2$ ($x = 0$, 0.1, 0.2, 0.3) semiconductors, the observed light absorption band-gap E_g is defined as a property criterion for selecting the two hybridization energy levels. The transition between the two energy levels should be determined after light absorption. Since the band-gap $E_g = 1.06$ eV (24.4436 kcal/mol) for $CuInTe_2$, the energy difference between the two selected hybridization energy levels should fit E_g well, that is, the relative error is within 10%. For selecting the two levels as shown in Table 7, the two hybridization states $\sigma = 3$, 4 are selected since the corresponding band-gaps are 342.8078 kcal/mole for $\sigma = 3$, and 319.9201 kcal/mole for $\sigma = 4$, respectively. Their energy difference is 22.9507 kcal/mol, which accords with the observed band-gap well. The valence electronic structures are listed in Table 11. The same calculations are performed for the other three $CuIn_{1-x}Eu_xTe_2$ semiconductors. The calculated valence electron structures are presented in Tables 11–14. Based on the above calculations, the diagram of hybrid electronic state transition induced by absorbing photons is shown as Figs. 2–5, where the symbols of $-$, $\bullet$, Φ, $\|$ denote covalent electrons, lattice electrons, and dumb pair electrons, respectively; s, p, d represent the relative electron numbers distributed in s, p, d orbitals.

Table 11. Valence electrons in the hybrid state of $CuInTe_2$.

Hybrid level	Cu	In	Te	Hybrid energy/kcal·mol^{-1}
$\sigma = 3$	13	10	1	342.8708
$\sigma = 4$	17	9	1	319.9201

Element	hybrid level	$n_c = n_s + n_p + n_d$			n_c	n_l	n_m	n_γ
		n_s	n_p	n_d				
Cu	13	0	2.7887	2.7887	5.5774	1	0	4.4226
	17	0	2.9958	2.9958	5.9916	1	0	4.0084
	Δ_1	0 –	0.2071 ↑	0.2071 ↑	0.4142 ↑	0 –	0 –	0.4142 ↓
In	10	1	3	1	5	0	0	8
	9	0.6399	2.6399	0.6399	3.9197	0.3601	0	8.7202
	Δ_2	0.3601 ↓	0.3601 ↓	0.3601 ↓	1.0803 ↓	0.3601 ↑	0 –	0.7202 ↑
$\Delta = \Delta_1 + \Delta_2$		0.3601 ↓	0.1530 ↓	0.1530 ↓	0.6661 ↓	0.3601 ↑	0 –	0.3060 ↑

Table 12. Valence electrons in the hybrid state of $CuIn_{0.9}Eu_{0.1}Te_2$.

Hybrid level	Cu	In	Te	Eu	Hybrid energy kcal/mol
$\sigma = 4$	15	10	1	1	342.6048
$\sigma = 5$	17	9	1	1	315.5869

Element	hybrid level	$n_c = n_s + n_p + n_d$			n_c	n_l	n_m	n_γ
		n_s	n_p	n_d				
Cu	15	0	2.9310	2.9310	5.8620	1	0	4.1380
	17	0	2.9958	2.9958	5.9916	1	0	4.0084
	Δ_1	0 –	0.0648 ↑	0.0648 ↑	0.1296 ↑	0 –	0 –	0.1296 ↓
In	10	1	3	1	5	0	0	8
	9	0.6399	2.6399	0.6399	3.9197	0.3601	0	8.7202
	Δ_2	0.3601 ↓	0.3601 ↓	0.3601 ↓	1.0803 ↓	0.3601 ↑	0 –	0.7202 ↑
$\Delta = \Delta_1 + \Delta_2$		0.3601 ↓	0.2593 ↓	0.2593 ↓	0.9507 ↓	0.3601 ↑	0 –	0.5906 ↑

Table 13. Valence electrons in the hybrid state of $CuIn_{0.8}Eu_{0.2}Te_2$.

Hybrid level	Cu	In	Te	Eu	Hybrid energy kcal/mol		
$\sigma=5$	17	10	1	1	340.8581		
$\sigma=4$	17	9	1	1	313.4229		
Element	hybrid level	$n_c=n_s+n_p+n_d$			n_c	n_l	n_m	n_γ
		n_s	n_s	n_s				
	17	0	2.9958	2.9958	5.9916	1	0	4.0084
Cu	17	0	2.9958	2.9958	5.9916	1	0	4.0084
	Δ_1	0 –	0 –	0 –	0 –	0 –	0 –	0 –
	10	1	3	1	5	0	0	8
In	9	0.6399	2.6399	0.6399	3.9197	0.3601	0	8.7202
	Δ_2	0.3601 ↓	0.3601 ↓	0.3601 ↓	1.0803 ↓	0.3601 ↑	0 –	0.7202 ↑
$\Delta=\Delta_1+\Delta_2$		0.3601 ↓	0.3601 ↓	0.3601 ↓	1.0803 ↓	0.3601 ↑	0 –	0.7202 ↑

Table 14. Valence electrons in the hybrid state of $CuIn_{0.7}Eu_{0.3}Te_2$.

Hybrid level	Cu	In	Te	Eu	Hybrid energy kcal/mol		
$\sigma=5$	17	10	1	1	330.7531		
$\sigma=2$	15	9	1	1	303.9720		
Element	hybrid level	$n_c=n_s+n_p+n_d$			n_c	n_l	n_m	n_γ
		n_s	n_s	n_s				
	17	0	2.9958	2.9958	5.9916	1	0	4.0084
Cu	15	0	2.9310	2.9310	5.8620	1	0	4.1380
	Δ_1	0 –	0.0648 ↓	0.0648 ↓	0.1296 ↓	0 –	0 –	0.1296 ↑
	10	1	3	1	5	0	0	8
In	9	0.6399	2.6399	0.6399	3.9197	0.3601	0	8.7202
	Δ_2	0.3601 ↓	0.3601 ↓	0.3601 ↓	1.0803 ↓	0.3601 ↑	0 –	0.7202 ↑
$\Delta=\Delta_1+\Delta_2$		0.3601 ↓	0.4249 ↓	0.4249 ↓	1.2099 ↓	0.3601 ↑	0 –	0.8498 ↑

As shown in Figs. 2–5, the light absorption induced electron transformations from covalent electron to lattice electron and from valance electron to dumb pair electron occur in an In atom. The increase of lattice electrons in lattice space is conducive to increasing the conductive ability and reducing resistivity, and the increase of dumb paired electrons causes the declination of the bonding energy for the CIET semiconductor.

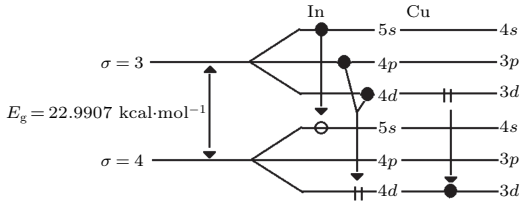


Fig. 2. Valence electronic state transition after absorbing photons of $CuInTe_2$.

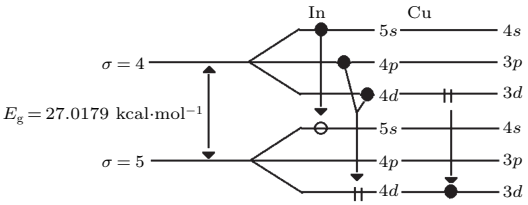


Fig. 3. Valence electronic state transition after absorbing photons of $CuIn_{0.9}Eu_{0.1}Te_2$.

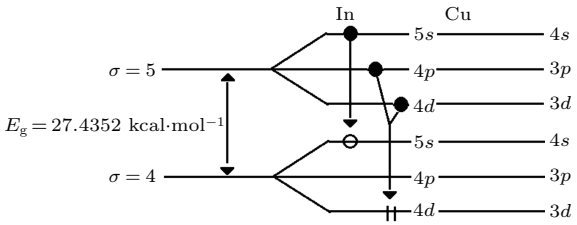


Fig. 4. Valence electronic state transition after absorbing photons of $CuIn_{0.8}Eu_{0.2}Te_2$.

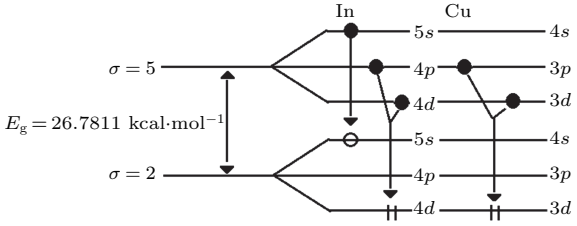


Fig. 5. Valence electronic state transition after absorbing photons of $CuIn_{0.7}Eu_{0.3}Te_2$.

For Cu atom, the electron transformation from dumb pair electron to covalent electron is observed after light absorption, which causes the increase of bonding energy. However, there is no change for Eu or Te. It implies that Eu doping into $CuInTe_2$ affects the valence electron structures of Cu and In

atoms. The hybridization states of Cu seem to be more sensitive to Eu doping. In single phase regimes of $x = 0$–0.2, Eu doping into $CuInTe_2$ causes electrons to transform from a dumb pair electron into a covalent electron, and reduce the bonding energy. However, the tendency of electron transformation is to cause the reverse result from the single phase solution region, i.e., the covalent electrons transformed into the dumb pair electron. The same transformation is also observed for the In atom. It reveals that Eu doping is helpful for improving the light performance of $CuInTe_2$ by adjusting the valence electron structures of Cu and In.

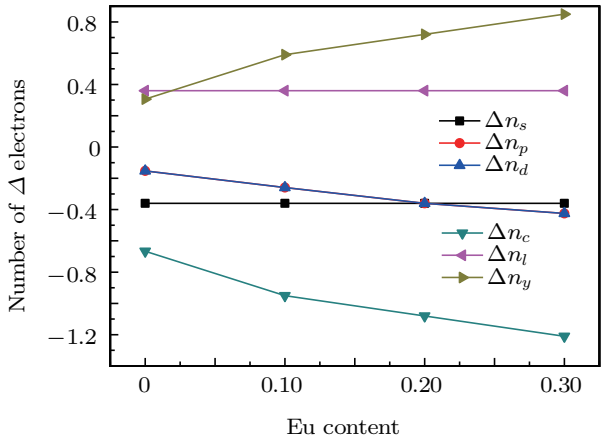


Fig. 6. (color online) Valence electronic changes of "Cu+In" for $CuIn_{1-x}Eu_xTe_2$ ($x = 0$, 0.1, 0.2, 0.3) series compounds.

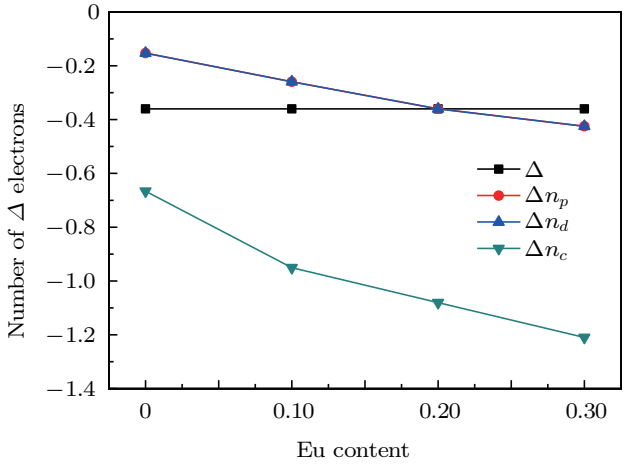


Fig. 7. (color online) Electronic charges s, p, d, n_c electronic changes of "Cu + In" for $CuIn_{1-x}Eu_xTe_2$ ($x = 0$, 0.1, 0.2, 0.3) series compounds.

Since the hybridization states of Cu and In are affected by Eu doping, the three figures (Figs. 6–8) are supplied for understanding the physical mechanism for optical performance of $CuInTe_2$ by Eu doping. The Eu doping into $CuInTe_2$ induces the covalent electrons n_c to decrease and the dumb pair electrons n_y to increase for Cu and In atoms with increasing the Eu doping content in the single phase region. For the In atom, its s covalent electrons are converted into lattice electrons n_l, and its p and d covalent electrons are converted into d dumb pair electrons with increasing Eu content; for the Cu atom, the electron transformation is influenced by Eu doping, and the covalent electrons transform into dumb pair electrons. The above-mentioned discussion reveals that the Eu doping has an effect on the band-gap width for each of $CuIn_{1-x}Eu_xTe_2$ semiconductors by adjusting 3d valence electrons of the Cu atom, and this adjusting action is helpful for improving the optical properties of $CuIn_{1-x}Eu_xTe_2$ semiconductors.

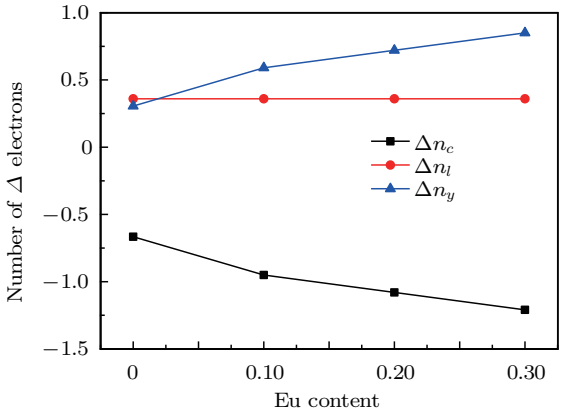


Fig. 8. (color online) Electronic charges n_c, n_l, n_y of "Cu + In" for $CuIn_{1-x}Eu_xTe_2$ ($x = 0$, 0.1, 0.2, 0.3) series compounds.

3. Conclusions

In this paper, the valence electron structures and bang-gaps of Eu-doped $CuIn_{1-x}Eu_xTe_2$ semiconductors are calculated systemically by the EET method. The theoretical calculations accord with experimental results well. The theoretical results show that Eu doping into $CuInTe_2$ mainly affects the valence electron structures of Cu and In atoms, and induces electron transformations from covalent electron to lattice electron and from valance electron to dumb pair electron after light absorption. The enlarged light absorption band gap is related to the increase of lattice electrons. It reveals the essential issue in the photoelectric affect is due to the change of valence electron structure induced by Eu doping.

Appendix A

The atomic state in a solid or a molecule is a hybridization of two atomic states, which can be called the h (head) and t (tail) states. At least one of them is the ground or near excited state. Both of them correspond to two stationary states, and a certain atomic state is the overlap of the two states. Both h and t states have their own numbers of covalent electrons n_c, "lattice electron" n_l, and the single bond radius $R(1)$.[30] The numbers of s, p, and d electrons are listed in hybridization tables of Cu, In, Te, and Eu as follows:

Table A1. Hybrid levels for Cu.

$3d^{10}4s \rightarrow 3d^8 4s4p'^2$,
$3d^{10}4p \rightarrow 3d^7 4s''4p'^3$,
$h \parallel \parallel \parallel \Phi_1 \bullet \bullet \Phi_l \underline{\cdot} \circ 1\ 2\ 2\ 0$
$l \parallel \parallel \bullet \bullet \bullet \Phi \underline{\cdot} \underline{\cdot} \underline{\cdot} 3\ 3\ 0\ z = 11$

σ	1	2	3	4	5	6	7	8	9
$C_h\sigma$	1	0.9999	0.9998	0.9983	0.9752	0.9502	0.9415	0.7997	07248
$C_t\sigma$	0	0.0001	0.0002	0.0017	0.0248	0.0498	0.0585	0.2003	0.2752
$n_T\sigma$	5	5.0002	5.0004	5.0034	5.0496	5.0996	5.1170	5.4006	5.5504
$n_l\sigma$	1	1	1	1	1	1	1	1	1
$n_c\sigma$	4	4.0002	4.0004	4.0034	5.0496	4.0996	4.1170	4.4006	4.5504
$R\sigma(1)$	1.1520	1.1520	1.1520	1.1520	1.1517	1.1513	1.1512	1.1492	1.1481
σ	10	11	12	13	14	15	16	17	18
$C_h\sigma$	0.6896	0.6601	0.5194	0.2113	0.1297	0.0690	0.0075	0.0042	0
$C_t\sigma$	0.3104	0.3399	0.4806	0.7887	0.8703	0.9310	0.9925	0.9958	1
$n_T\sigma$	5.6208	5.6798	5.9612	6.5774	6.7406	6.8620	6.9850	6.9916	7
$n_l\sigma$	1	1	1	1	1	1	1	1	1
$n_c\sigma$	4.6208	4.6798	4.9612	5.5774	5.7406	5.8620	5.9850	5.9916	6
$R\sigma(1)$	1.1477	1.1472	1.1453	1.1410	1.1398	1.1390	1.1381	1.1381	1.1380

Table A2. Hybrid levels for In.

$4d^{10}5s5p^2 + 4d^{10}5s5p^2 \rightarrow 4d^9 5s5p^2 5p'$,
$h \parallel \parallel \parallel \parallel \parallel \Phi \bullet \bullet \circ 1\ 2\ 0\ 0$
$t \parallel \parallel \parallel \parallel \bullet \bullet \bullet \bullet \bullet 1\ 3\ 1\ 1\ z = 13$

σ	1	2	3	4	5	6	7	8	9	10
$C_h\sigma$	1	0.9996	0.9975	0.9755	0.8755	0.8735	0.7612	0.5495	0.3601	0
$C_t\sigma$	0	0.0004	0.0025	0.0245	0.1245	0.1265	0.2388	0.4505	0.6399	1
$n_T\sigma$	3	3.0008	3.0050	3.0490	3.2490	3.2530	3.4776	3.9010	4.2798	5
$n_l\sigma$	1	0.9996	0.9975	0.9755	0.8755	0.8735	0.7612	0.5495	0.3601	0
$n_c\sigma$	2	2.0012	2.0075	2.0735	2.3735	2.3795	2.7164	3.3515	3.9197	5
$R\sigma(1)$	1.4420	1.4420	4.4418	1.4404	1.4339	1.4338	1.4265	1.4127	1.4004	1.3770

Table A3. Hybrid Levels for Te.

$h \bullet \parallel \parallel \bullet 1\ 1\ 0\ 1$
$t \parallel \parallel \bullet \bullet 0\ 2\ 0\ 1$

σ	1	2	3	4
$C_h\sigma$	1	0.5544	0.0820	1
$C_t\sigma$	0	0.4456	0.9180	1
$n_T\sigma$	2	2	2	2
$n_l\sigma$	0	0	0	0
$n_c\sigma$	2	2	2	2
$R\sigma(1)$	1.313	1.4194	1.531	1.550

Table A4. Hybrid Levels for Eu.

$s'p'd'$ $h \bullet \circ \circ \circ \circ \Phi \bullet \circ \circ 1\ 1\ 1\ 0$
$s;d^2$ $l \circ \circ \circ \circ \circ \bullet \bullet \bullet \circ 1\ 0\ 2\ 1\ z = 3$

$$k = \frac{3}{2}\frac{1 \pm \sqrt{3} \pm \sqrt{5}}{1 \pm \sqrt{6}} \quad z' = 8$$

σ	1	2	3	4	5	6	7	8	9	10
$C_h\sigma$	1	0.9635	0.9042	0.8235	0.7078	0.6249	0.2996	0.2085	0.0444	0
$C_t\sigma$	0	0.0365	0.0958	0.1765	0.2922	0.3751	0.7004	0.7915	0.9556	1
$n_T\sigma$	3	3	3	3	3	3	3	3	3	3
$n_l\sigma$	1	0.9635	0.9042	0.8235	0.7078	0.6249	0.2996	0.20857	0.0444	0
$n_c\sigma$	2	2.0365	2.0958	2.1765	2.2922	2.3751	2.7004	2.7915	2.9556	3
$R\sigma(1)$	1.4691	1.4820	1.5031	1.5318	1.5729	1.6024	1.7179	1.7503	1.8086	1.8244

The theoretical model for calculating the crystalline cohesive energy was given first by Yu[27] in empirical electron theory (EET), and the crystalline cohesive energy $\overline{E_C}$ is expressed as follows:

$$\overline{E_C} = b\left\{\sum_\alpha \frac{I_\alpha n_\alpha}{D_{(n_\alpha)}} f + \frac{n_l}{\overline{D}} f' + am^{3d} - CW\right\}, \tag{A1}$$

where $b = 75/(n - 0.36\delta)$ (kcal·Å/mol) with $n = 1$, 2, 3, 4, 5, 7 or 13, $\delta = 2$, 1, 0: for the elements in this study, their b (kcal·Å/mol) values are 20.6044 for Cu, 32.894 for In, 37.500 for Te, 45.7317 for Eu; I_α, n_α, and $D(n_\alpha)$ represent the bond number, the number of bonding electron pairs, and bond distance of α bond; f and f' represent the abilities of covalent electron and crystalline electron to form bonds; $\overline{D}$ is the equivalent bond distance and expressed as $\overline{D} = \sum I_\alpha D_{(n\alpha)} / \sum I_\alpha$, with referring to covalent bonds around lattice electrons, $f' = \sqrt{2\alpha'}$ denotes the bonding capability of lattice electrons, and $\alpha' = n_\alpha / n_T$, with n_T being the total number of valence electrons.[2]

$a = 0.1542$, $C = 0.907P$, for elements in V, VI, VII of B subfamily, Fe, Co, Ni in VIII, elements in BI, BII, their P values are in the order of 6, 5, 4, 3, 2, 1, and 0 (0 for BI, BII),

$$W = \frac{\text{magnetic elections + dumb pair electrons}}{\text{total number of electrons}}. \tag{A2}$$

Empirical electron theory only supplies P values of B group elements, and therefore the binding energies of the A group elements containing dumb pair electrons need calculating with an appropriate guess and speculation. In this paper, we suppose that the P value of Cu is 0; the rare earth element Eu belongs to the III B group, so that the P value is 0; In and Te are the A group elements, whose P values are both 0. The calculation is carried out based on those conditions.

The formula for calculating the binding energy of a compound crystal is[33,34]

$$\begin{aligned}\overline{E_C^0} = {} & \sum_\alpha \overline{B_\alpha} \frac{I_\alpha n_\alpha}{D_{(n_\alpha)}} \overline{F_\alpha} + \overline{B_l} \frac{n_l}{\overline{D}_{(n_l)}} f' + b_u a m^{3d} \\ & - b_u CW + b_v a m^{3d} - b_v CW,\end{aligned} \tag{A3}$$

where

$$\overline{B_\alpha} = \sqrt{b_u b_v} \quad \alpha = A, B, \tag{A4}$$

with an α bond being formed between u and v atoms;

$$\overline{B_l} = \sqrt[m+n]{b_u^m b_v^n}, \tag{A5}$$

with m and n denoting the numbers of u and v atoms, respectively, in molecular formula;

$$\overline{F_\alpha} = \frac{1}{2}(f_u + f_v), \tag{A6}$$

with f_u and f_v denoting the bonding capabilities of u and v atoms when they form the α bond; and b_u and b_v refer to the shielding coefficient (b) values of u and v crystalline binding energy, respectively.

References

[1] Abo El Soud A M, Zayed H A and Soliman L I 1993 *Thin Solid Films* **229** 232

[2] Bhattacharya R N and Rajeshwar K 1986 *Solar Cells* **16** 237

[3] Gonzalez J and Rincón C 1990 *J. Phys. Chem. Solids* **51** 1093.

[4] Hörig W, Neumann H and Godmanis I 1980 *Solid State Commun.* **36** 181

[5] Kazmerski L L and Shieh C C 1977 *Thin Solid Films* **41** 35

[6] Cao M, Men C L, Zhu D M, *et al.* 2013 *Chin. Phys. B* **22** 107803

[7] Gu Y N, Xu S and Wu X S 2016 *Chin. Phys. B* **25** 123103

[8] Sugan S, Baskar K and Dhanasekaran R 2014 *Curr. Appl. Phys.* **14** 1416

[9] Bagci S, Yalcin B G, Aliabad H A R, Duman S and Salmankurt B 2016 *Rsc Adv.* **6** 59527

[10] Boustani M, El Assali K, Bekkay T and Khiara A 1997 *Solar Energy Mater. Solar Cells* **45** 369

[11] Hadi Zarei and Rasoul Malekfar 2016 *Chin. Phys. B* **25** 027103

[12] Merabet B, Alamri H, Djermouni M, Zaoui A, Kacimi S, Boukortt A, *et al.* 2017 *Chin. Phys. Lett.* **34** 016101

[13] Lakhe M and Chaure N B 2014 *Solar Energy Mater. Solar Cells* **123** 122

[14] Mahalingam T, Thanikaikarasan S, Sanjeeviraja C, Kim T, Sebastian P J and Kim Y D 2010 *J. New Mater. Electrochem. Syst.* **13** 77

[15] Mise T and Nakada T 2012 *J. Vac. Sci. Technol. A* **30** 324

[16] Fu L and Guo Y Q 2014 *Chin. Phys. B* **23** 127801

[17] Valeri-Gil M L and Rincón C 1993 *Mater. Lett.* **17** 59

[18] Cheng N, Liu R, Bai S, Shi X and Chen L 2014 *J. Appl. Phys.* **115** 894

[19] Hervé P and Vandamme L K J 1994 *Infr. Phys. Technol.* **35** 609

[20] Mitzi D B, Copel M and Murray C E 2006 *Adv. Mater.* **18** 2448

[21] Orts J L, Diaz R, Herrasti P, Rueda F and Fatas E 2007 *Solar Energy Mater. Solar Cells* **91** 621

[22] Mi S 2009 "Study on Semiconductor CuXTe$_2$ (X = Ga, In) and ZnGa_2X_4 (X = S, Se) based on first principle", MS. Ddissertation (Taiyuan: Shanxi University) (in Chinese)

[23] Li Y P, Meng Q S, Deng Y, Zhou H, Gao Y L, Li Y Y, *et al.* 2012 *Appl. Phys. Lett.* **100** 231903

[24] Aissaoui O, Mehdaoui S, Bechiri L, Benabdeslem M, Benslim N, Amara A, *et al.* 2011 *J. Lumin.* **131** 109

[25] Nie X M and Guo Y Q 2016 *J. Solid State Chem.* **233** 211

[26] Sanad M M S, Rashad M M and Shenouda A Y 2016 *Int. J. Electrochem. Sci.* **11** 4337

[27] Yu R H 1978 *China Academic Journal Electronic Publishing House* **23** 217 (in Chinese)

[28] Meng Z H, Fu L, Mei J, *et al.* 2013 *Sci. Sin.-Phys. Mech. Astron.* **43** 275

[29] Wu W X, Guo Y Q, Li A H and Li W 2008 *Acta Phys. Sin.* **57** 2486 (in Chinese)

[30] Guo Y Q, Yu R H, Zhang R L, *et al.* 1998 *J. Phys. Chem. B* **102** 9

[31] Li Z L, Xu H B and Gong S K 2004 *J. Phys. Chem. B* **108** 15165

[32] Lu J Z snd Wang S K 1979 *China Academic Journal Electronic Publishing House* **24** 724 (in Chinese)

[33] Meng Z H, Li J B, Guo Y Q and Wang Y 2012 *Acta Phys. Sin.* **61** 107101 (in Chinese)

[34] Zhang R L 1993 *The Empirical Electron Theory of Solids and Molecules* (Changchun: Jilin Science and Technology Press) (in Chinese)